Active Vibration Isolation of Multiple Degree-of-Freedom System based on the Minimization of the Output Force Control Strategy

Song Chunsheng[1,a], Hu Yefa[1,b]
[1]School of Mechanical and Electronic Engineering, Wuhan University of Technology, Wuhan 430070, China
[a]song_chsh@163.com, [b]huyefa@whut.edu.cn

Abstract: Vibration isolation technology has been widely used to reduce the vibration transmission from the machinery to the foundation in many different engineering systems. Magnetic suspension vibration isolation technology is an excellent active isolation technology, which has some useful characteristics, such as non-contact, high response frequency, high reliability and long life-span. Hence, the magnetic suspension isolator is designed. The electromagnetic force of the magnetic suspension active isolator is measured in advance by experiment. Multiple degrees of freedom (DOFs) vibration isolation system supported by magnetic suspension isolators and springs is established. The dynamical and state equations of the system are formulated. A control algorithm and the value function of active vibration isolation based on force transmissibility are proposed. The control model based on the control algorithm is established. Output force responses of the active vibration isolation system and passive one under same excitation are simulated. The simulation results indicate the active system possessed much better effect on vibration isolation. Comparing with passive system, the force transmissibility is reduced by 2dB-3dB in low-frequency stage, especially around resonance frequency, the transmissibility is reduced by 10dB-18dB. In order to test the reliability of the active system and control algorithm, an experimental platform is carried out. Experiment results show that the force transmissibility is reduced by 10dB-15dB around resonance frequency. The research indicates that experimental results are found to be in good agreement with simulated results.

Keywords: Magnetic Suspension Isolator, Minimization of the Output Force, Active Vibration Isolation, Control Strategy

1 Introduction

In recent years, vibration isolation systems have been studied broadly and in great depth [1].Vibration isolation technology has been widely used to reduce the vibration transmission from the machinery to the foundation in many different engineering systems. It can be classified into two types: passive and active. Although the passive one offers simple and reliable means to protect mechanical systems from a vibration environment, it has inherent performance limitations, that is, its controllable frequency range is limited and the shape of its transmissibility does not change. On the other hand, active vibration isolation systems, with parameters that change according to excitation and response characteristics of the system can provide significantly enhanced vibration isolation performance [2].Many active control strategies have been proposed to provide effective vibration control[3-6,15].

Magnetic suspension supporting technology is a new supporting technology developed from later period of last century ,which has the characteristic of controllability and adjustability, especially, the damping and stiffness adjusted by changing controls parameters on-line[7-8].With the technology，magnetic suspension isolator is an excellent active isolator. which has some useful characteristics, such as non-contact, high response frequency, high reliability, long life-span and etc, so there were some studies about the organization and

character of itself and its application[9-10], such as the “Smart Spring” [11-12].

However, most of the these are by means of the theoretical formula of electromagnetic force to do some simulations. But there are large differences between the theoretical and actual expression[13-14], As a result of many assumptions of theoretical formula which ignores saturation and flux leakage and the coupling to magnetic field. Moreover, the thickness of air-gap of the isolator is larger than normal magnetic suspension system such as magnetic bearings. The difference between theory and practice should be greater. So, the simulation result may not very agree with the fact.

To solve the problem, the magnetic suspension isolator is designed firstly, and the characteristics and capacity of the isolator are studied experimentally and theoretically. The electromagnetic force of the magnetic suspension active isolator is measured in advance by experiment. Through the data experimental measurement and fitting a mathematical expression by least square method, the actual relation expression of electromagnetic force-current-gap is obtained. A control mechanism and the cost function of active vibration isolation based on minimization of force transmissibility are proposed. Secondly, the computer simulation and experiment are carried out. A comparison between the simulation and experimental results is obtained. Finally, the result and conclusion has been given.

2 The model of magnetic suspension Multiple DOFs active isolation system

2.1 Mathematical model

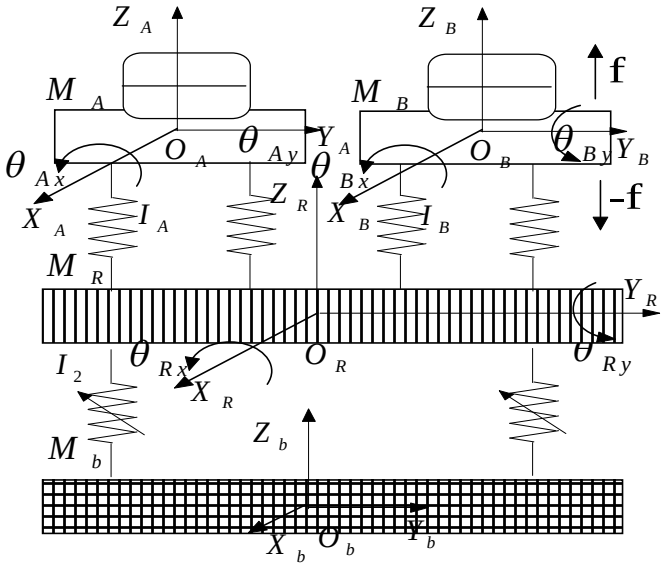

Figure 1 The active isolation system

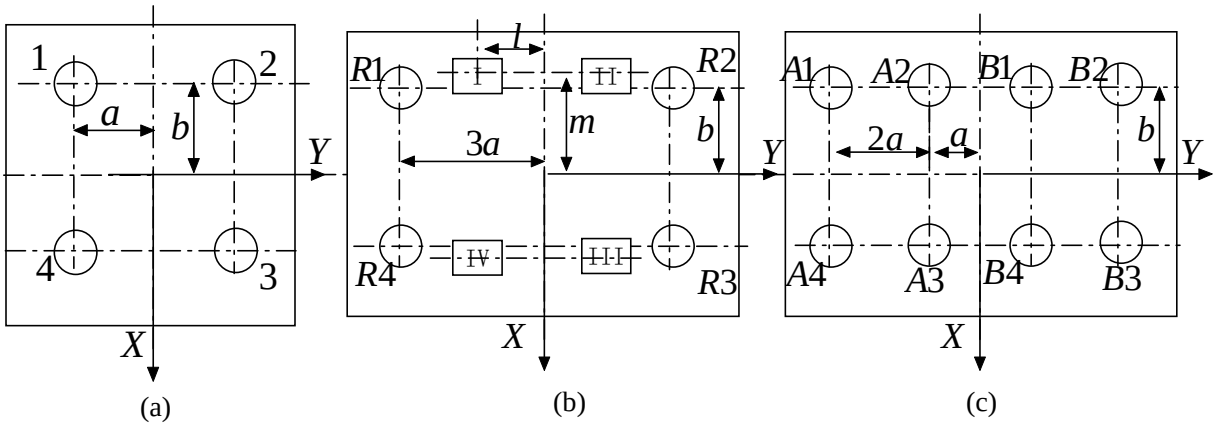

Figure2. Distribution map of isolators in isolation tables and middle raft
(a) distribution map of M_A and M_B; (b),(c) distribution map of M_R

Fig.1 shows the structure of Multiple Dofs vibration isolation system with magnetic suspension isolators. It has two isolation tables (M_A, M_B), a middle raft (M_R), and a base (M_b). The four magnetic suspension isolators are fixed between the middle and base. The middle raft is supported by four magnetic suspension isolators and four ordinary springs I_R. Each isolation table is supported by four ordinary springs respectively.

The projection the isolation tables and middle raft are shown in Figure .2 (a, b), so the isolators' positions are determined. 1, 2, 3 and 4 shown in Figure 2-a are the positions of the upper springs on M_A, M_B. A1, A2, A3, A4 B1, B2, B3 and B4 are the positions of upper springs on middle raft. Ⅰ, Ⅱ, Ⅲ and Ⅳ shown in Figure 2-b are the positions of magnetic suspension isolators. R1, R2, R3 and R4 shown in Figure 2-b are the positions of lower springs on middle raft. $Z_AO_AY_A$, $Z_BO_BY_B$, $Z_RO_RY_R$ and $Z_bO_bY_b$ are rectangular Cartesian coordinate systems of M_A , M_R and M_b shown in Figure 1. There are three DOFs: one translational motion in the vertical direction (Z) and two rotational motions, roll (Θ_x) and pitch (Θ_y).Considering practical situation, it is assumed that the roll and pitch angles are so small (≤2.5°) that $\cos\theta_{kx} \cong 1, \sin\theta_{kx} \cong \theta_{kx}$, $\cos\theta_{ky} \cong 1$, *and* $\sin\theta_{ky} \cong \theta_{ky}$, where, θ_{kx}, θ_{ky} are the roll and pitch angles of the isolation object M_A, M_B, M_R and M_b.(k=A ,B, R).

(1) Dynamical equation

The dynamic mathematic equation motion of the isolation M_A is

$$\begin{cases} m_A\ddot{z}_A = -4k_A^u z_A + 4k_A^u(z_R - 2a\theta_{Rx}) - 4c_A^u\dot{z}_A + 4c_A^u(\dot{z}_R - 2a\dot{\theta}_{Rx}) + f_A^d \\ J_{Ax}\ddot{\theta}_{Ax} = -4a^2k_A^u\theta_{Ax} + 4a^2k_A^u\theta_{Rx} - 4a^2c_A^u\dot{\theta}_{Ax} + 4a^2c_A^u\dot{\theta}_{Rx} + m_{Ax}^d \\ J_{Ay}\ddot{\theta}_{Ay} = -4b^2k_A^u\theta_{Ay} + 4b^2k_A^u\theta_{Ry} - 4b^2c_A^u\dot{\theta}_{Ay} + 4b^2c_A^u\dot{\theta}_{Ry} + m_{Ay}^d \end{cases} \quad (1)$$

The dynamic mathematic equation motion of the isolation M_B is

$$\begin{cases} m_B\ddot{z}_B = -4k_B^u z_B + 4k_B^u(z_R + 2a\theta_{Rx}) - 4c_B^u\dot{z}_B + 4c_B^u(\dot{z}_R + 2a\dot{\theta}_{Rx}) + f_B^d \\ J_{Bx}\ddot{\theta}_{Bx} = -4a^2k_B^u\theta_{Bx} + 4a^2k_B^u\theta_{Rx} - 4a^2c_B^u\dot{\theta}_{Bx} + 4a^2c_B^u\dot{\theta}_{Rx} + m_{Bx}^d \\ J_{By}\ddot{\theta}_{By} = -4b^2k_B^u\theta_{By} + 4b^2k_B^u\theta_{Ry} - 4b^2c_B^u\dot{\theta}_{Ay} + 4b^2c_B^u\dot{\theta}_{Ry} + m_{By}^d \end{cases} \quad (2)$$

The dynamic mathematic equation motion of the isolation M_R is

$$\begin{cases} m_R\ddot{z}_R = \sum_{i=I}^{IV} F_i + 4k_A^u z_A - 4k_A^u(z_R - 2a\theta_{Rx}) + 4c_A^u\dot{z}_A - 4c_A^u(\dot{z}_R - 2a\dot{\theta}_{Rx}) + 4k_B^u z_B - 4k_B^u(z_R + 2a\theta_{Rx}) \\ +4c_B^u\dot{z}_B - 4c_B^u(\dot{z}_R + 2a\dot{\theta}_{Rx}) - 4k^d z_R + k^d(z_{b1} + z_{b2} + z_{b3} + z_{b4}) - 4c^d\dot{z}_R + c^d(\dot{z}_{b1} + \dot{z}_{b2} + \dot{z}_{b3} + \dot{z}_{b4}) \\ J_{Rx}\ddot{\theta}_{Rx} = -l(F_I - F_{II} + F_{III} - F_{IV}) - 8ak_A^u z_A + 4a^2k_A^u\theta_{Ax} + 8ak_A^u z_R - 20a^2k_A^u\theta_{Rx} - 8ac_A^u\dot{z}_A + 4a^2c_A^u\dot{\theta}_{Ax} + \\ 8ac_A^u\dot{z}_R - 20a^2c_A^u\dot{\theta}_{Rx} + 8ak_B^u z_B - 4a^2k_B^u\theta_{Bx} - 8ak_B^u z_R - 20a^2k_B^u\theta_{Rx} + 8ac_B^u\dot{z}_B \\ -4a^2c_B^u\dot{\theta}_{Bx} - 8ac_B^u\dot{z}_R - 20a^2c_B^u\dot{\theta}_{Rx} - 36a^2k^d\theta_{Rx} - 3ak^d(z_{b1} - z_{b2} + z_{b3} - z_{b4}) - 36a^2c^d\dot{\theta}_{Rx} \\ -3ac^d(\dot{z}_{b1} - \dot{z}_{b2} + \dot{z}_{b3} - \dot{z}_{b4}) \\ J_{Ry}\ddot{\theta}_{Ry} = m(F_I + F_{II} - F_{III} - F_{IV}) + 4b^2k_A^u\theta_{Ay} - 4b^2k_A^u\theta_{Ry} + 4b^2c_A^u\dot{\theta}_{Ay} - 4b^2c_A^u\dot{\theta}_{Ry} + 4b^2k_B^u\theta_{By} - \\ 4b^2k_B^u\theta_{Ry} + 4b^2c_B^u\dot{\theta}_{By} - 4b^2c_B^u\dot{\theta}_{Ry} - 4b^2k^d\theta_{Ry} + bk^d(z_{b1} + z_{b2} - z_{b3} - z_{b4}) - 4b^2c^d\dot{\theta}_{Ry} \\ +bc^d(\dot{z}_{b1} + \dot{z}_{b2} - \dot{z}_{b3} - \dot{z}_{b4}) \end{cases} \quad (3)$$

Where,

m_A is the mass of the isolation table M_A;
m_B is the mass of the isolation table M_B;
m_R is the mass of the middle raft M_R;
J_{Ax} is the inertial momentum of the isolation table M_A about x-axis;
J_{Ay} is the inertial momentum of the isolation table M_A about y-axis;
J_{Bx} is the inertial momentum of the isolation table M_B about x-axis;
J_{By} is the inertial momentum of the isolation table M_B about y-axis;
$J_{R\,x}$ is the inertial momentum of the middle raft M_R about x-axis;
$J_{R\,y}$ is the inertial momentum of the middle raft M_B about y-axis;
F^d_A is the z-direction direct disturbance of M_A;
m^d_{Ax} is the direct disturbance about the x-axis of M_A;
m^d_{Ay} is the direct disturbance about the y-axis of M_A;
F^d_B is the z-direction direct disturbance of M_B;
m^d_{Bx} is the direct disturbance about the x-axis of M_B;
m^d_{By} is the direct disturbance about the y-axis of M_B;
z_A is the displacement of the center of the isolation table M_A;
z_B is the displacement of the center of the isolation table M_B;
z_R is the displacement of the center of the isolation table M_R;
F_{ke} is the z-direction electromagnetic force (k=I, II, III);
k^u_A is the stiffness of I_A;
k^u_B is the stiffness of I_B;
k_d is the stiffness of I_R;
c^u_A is the damping of I_A;
c^u_B is the damping of I_B;

(2)Equation of state

According to the equation (1) and (2) ,The state equation is established,
(1)The state variables are,

$$X=[v_1,v_2,v_3,v_4,v_5,v_6,v_7,v_8,v_9,v_{10},v_{11},v_{12},v_{13},v_{14},v_{15},v_{16},v_{17},v_{18}]^T=$$
$$[z_A,\theta_{Ax},\theta_{Ay},\dot{z}_A,\dot{\theta}_{Ax},\dot{\theta}_{Ay},z_B,\theta_{Bx},\theta_{By},\dot{z}_B,\dot{\theta}_{Bx},\dot{\theta}_{By},z_R,\theta_{Rx},\theta_{Ry},\dot{z}_R,\dot{\theta}_{Rx},\dot{\theta}_{Ry}]^T$$

(2)The control variables are,

$$U=[u_1,u_2,u_3,u_4]^T=[F_{Ie},F_{IIe},F_{IIIe},F_{IVe}]^T$$

(3)The input are the disturbing force and moment F,

$$F=[f_1,f_2,f_3,f_4,f_5,f_6]^T=[f_A^d,m_{Ax}^d,m_{Ay}^d,f_B^d,m_{Bx}^d,m_{By}^d]^T$$

(4)The output are the forces which transfer to the base ,including two part: spring force and magnetic force , $Y=[F_1^d,F_2^d,F_3^d,F_4^d,F_{Ie},F_{IIe},F_{IIIe},F_{IVe}]^T$, where， F_i^d (i=1，2，3，4)is the lower spring force。

(5)Assuming that the base is rigid and fixed on the ground, namely, $\delta_b=[z_{b1},z_{b2},z_{b3},z_{b4}]^T=O$,then the state equation is,

$$\begin{cases}\dot{X}=AX+BU+EF\\ Y=CX+DU\end{cases} \tag{4}$$

The value of the five matrices *A,B,C,D and E* (See Appendix **A**.).

2.2 Structure and parameters

The structure of the magnetic suspension isolator is shown in Fig.3, contains: 1. magnetic suspension bracket, 2.E-shape magnet, 3. coil, 4. displacement sensor and 5. armature and so on.

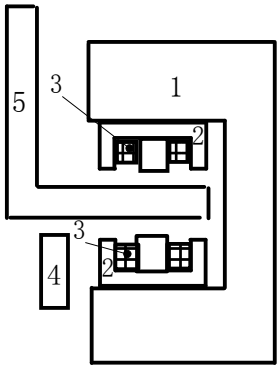

Figure 3 Structure of magnetic suspension isolator

The actual expression of electromagnetic force has been achieved in the help of the method of least square by the experimental Data[16].

$$F=\frac{870\cdot i_1^2}{x^2}-\frac{680\cdot i_2^2}{(8.6-x)^2} \tag{5}$$

i_1 and i_2 are currents of upper and lower coils

3 The control model of the system

The minimization of the sum of weighted squared output forces is as the cost function. The output forces are composed of two parts: lower spring force F^d , magnetic force F^e , N_D is the number of the lower springs and N_{MD} is the number of the MSIs.

$$F_{out} = \sum_{i=1}^{N_D} F_i^d(t) + \sum_{j=1}^{N_{MD}} F_j^e(t) \tag{6}$$

The cost function of the system is,

$$J = \int_0^\infty [q_1 \left(F_1^d\right)^2 + q_2 \left(F_2^d\right)^2 + \cdots + q_i \left(F_i^d\right)^2 + \cdots + q_{N_D} \left(F_{N_D}^d\right)^2 + q_{N_D+1} \left(F_1^e\right)^2 + q_{N_D+2} \left(F_2^e\right)^2 + \cdots + q_{N_D+j} \left(F_j^e\right)^2 + \cdots + q_{N_D+N_{MD}} \left(F_{N_{MD}}^e\right)^2]dt \tag{7}$$

$q_1, q_2 \ldots q_i \ldots q_{N_D} \ldots q_{N_D+j} \ldots q_{N_D+N_{MD}}$ are weighting coefficient.

Given the capacity of the magnetic isolators, the cost function is corrected to ,

$$J' = \int_0^\infty [q_1 \left(F_1^d\right)^2 + q_2 \left(F_2^d\right)^2 + \cdots + q_i \left(F_i^d\right)^2 + \cdots + q_{N_D} \left(F_{N_D}^d\right)^2 + q_{N_D+1} \left(F_1^e\right)^2 + q_{N_D+2} \left(F_2^e\right)^2 + \cdots + q_{N_D+j} \left(F_j^e\right)^2 + \cdots + q_{N_D+N_{MD}} \left(F_{N_{MD}}^e\right)^2 + r_1 U_1{}^2 + r_2 U_2{}^2 + \cdots + r_j U_j{}^2 + \cdots + r_{N_{MD}} U_{MD}{}^2]dt \tag{8}$$

$q_1, q_2 \ldots q_i \ldots q_{N_D} \ldots q_{N_D+j} \ldots q_{N_D+N_{MD}}$ are weighting coefficient; $U_1, U_2 \ldots U_{MD}$ are the control forces.

$r_1 \ldots r_j \ldots r_{N_{MD}}$ are weighting coefficient for control force. the larger weighting coefficient , the higher control force, and vice versa.

Subject to $Q_1 = diag\{q_1, q_2 \ldots q_i \ldots q_{N_D} \ldots q_{N_D+j} \ldots q_{N_D+N_{MD}}\}, R_1 = diag\{r_1 \ldots r_j \ldots r_{N_{MD}}\}$ 。

According to equation(3),

$$q_1 \left(F_1^d\right)^2 + q_2 \left(F_2^d\right)^2 + \cdots + q_i \left(F_i^d\right)^2 + \cdots + q_{N_D} \left(F_{N_D}^d\right)^2 + q_{N_D+1} \left(F_1^e\right)^2 + q_{N_D+2} \left(F_2^e\right)^2 + \cdots + q_{N_D+j} \left(F_j^e\right)^2 + \cdots + q_{N_D+N_{MD}} \left(F_{N_{MD}}^e\right)^2 = Y^T Q_1 Y$$
$$r_1 U_1{}^2 + r_2 U_2{}^2 + \cdots + r_j U_j{}^2 + \cdots + r_{N_{MD}} U_{MD}{}^2 = U^T R_1 U \tag{9}$$

And,

$$Y^T Q_1 Y = X^T C^T Q_1 C X + 2X^T C^T Q_1 D U + U^T (R_1 + D^T Q_1 D) U$$

$$Y^T Q_1 Y = X^T Q X + 2X^T N U + U^T R U$$

Where,

$$Q = C^T Q_1 C; \quad N = C^T Q_1 D; \quad R = R_1 + D^T Q_1 D$$

Where, the two matrices *C,D* can be obtain for equation(3),
Then cost function has the form :

$$J^{'} = \int_0^{\infty} (X^T QX + 2X^T NU + U^T RU)\ dt \tag{10}$$

Where,

$$Q = C^T Q_1 C;\ \ N = C^T Q_1 D;\ \ R = R_1 + D^T Q_1 D$$

According to extremum principle, control force is confirmed,

$$U = -R^{-1}(N^T + B^T P)X = -GX$$

Where,
G is the optimal control gain matrix, *P* is the solution of Riccati Equations

$$PA + A^T P - PBR^{-1}B^T P + Q = 0$$

By calculating, we can see that the closed-loop system is stable.

4 Simulation analysis and results

According to the dynamic mathematic Equations and control model established, the active control model is simulated though MATLAB/SINULINK6.5 platform. The parameter values used for the simulation are given as M_A=105.2kg，J_{Ax}=7.00kg*m^2， J_{Ay}=8.02kg*m^2; M_B=105.2kg， J_{Bx}=7.00kg*m^2， J_{By} =8.02kg*m^2； M_R=675.7kg， J_{Rx}=129.73kg*m^2， J_{RZ}=69.15kg*m^2； $K_A^u = 120N/mm$， $c_A^u = 50.24$N*s/m， $K_B^u = 60N/mm, c_B^u = 35.53$N*s/m， $K^d = 450N/mm, c^d = 243.3$N*s/m， l=0.6;m=0.4;a=0.3;b=0.3; From these parameters, we can get the main resonant vibration frequencies of the no control system are about：6.4Hz，8.3Hz and 12.0Hz.

The input force signal is taken to be chirp signal, and the range of the frequency is from 0.1Hz to 40Hz, the value of amplitude is 400N. The input torques signal is constant value ,M_x=100Nm,M_y=100Nm.

According to the performance of isolation and the capacity of magnetic suspension isolator， $Q_1 = diag(10,10,10,10,10,10,10,10)$ and $R_1 = diag(40,40,40,40)$。

The initial upper coils' and lower coils' currents of magnetic isolator are 2A. The time of simulation is 4s.

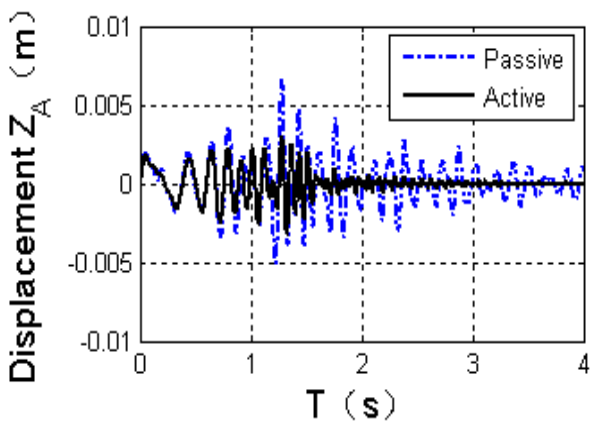

Figure 4 M_A 's Z-displacement of the systems

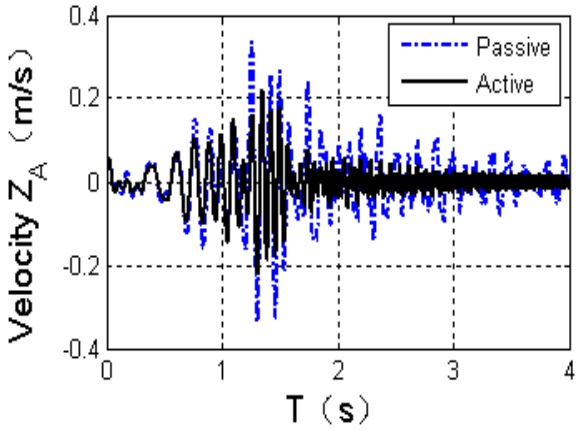

Figure 5 M_A 's Z-Velocity of the systems

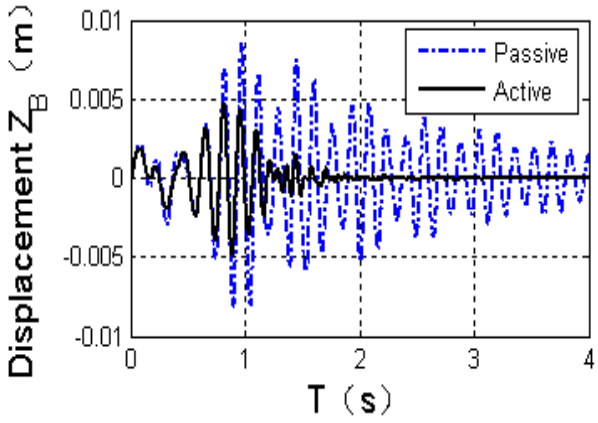

Figure 6 M_B 's Z-displacement of the systems

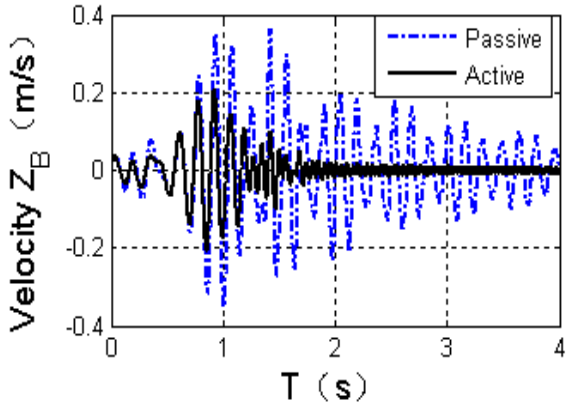

Figure 7 M_B 's Z-velocity of the systems

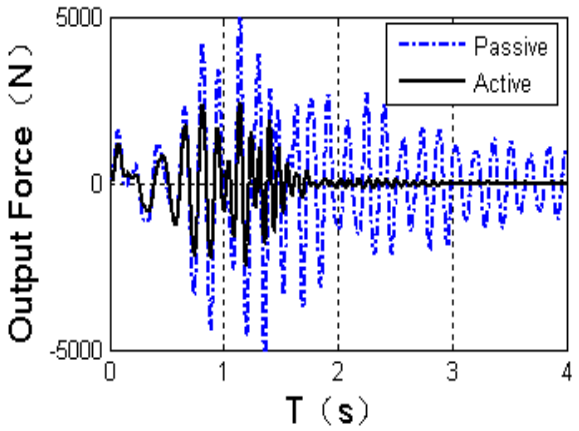

Figure 8. Output Forces of the systems

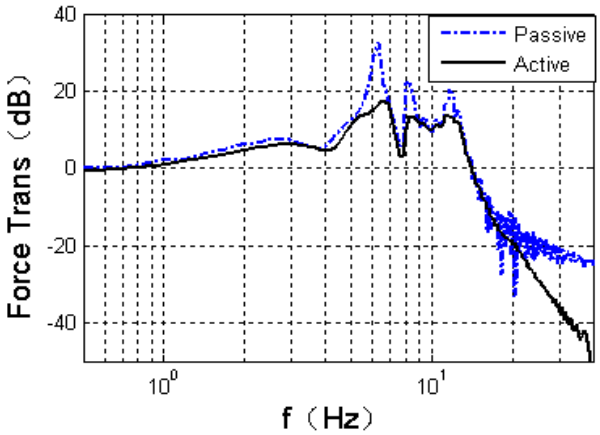

Figure 9. Force transmissibility of the systems

Under the same input signals, Fig.4, Fig.5, Fig.6 and Fig.7 shows the output Z-displacement and Z-velocity of the isolation table M_A , the dashed line denotes the passive system, while the real line denotes the active isolation system. It is evident that the M_A and M_B 's Z-displacement displacement and Z-velocity of active system is far smaller than the passive system all the time, especially around resonance frequencies, the maximum value of

active one is just is less than half of the past system..

The force transmissibility is the important method to evaluate system's isolation effectiveness. The output forces of the two systems are shown in Fig.8 ; the dashed line denotes the passive system, while the real line denotes the active isolation system. we can see that the output force of the active system is much smaller than the passive one, most of time the value of active is less than one third of passive system.

According to the two force transmissibility curves both active and passive system show in Fig.9. We can see the active curve is 2-3dB lower the passive one in most low frequency. The isolation performance remarkably enhance 10-18dB around resonance frequency. The active also possess a good isolation performance comparing with the passive at high frequency domain. Based on the results of simulate, the active vibration isolation system has much better isolating performance in a very broad frequency range, especially, at resonant frequencies.

5 Experiment research

Simulation results show that magnetic suspension active system based on strategy of minimum force transmissibility has much better performance of vibration isolation than passive one. In order to prove the results of the Simulation, a platform is built, which is showed in Fig.11 . By the action of guide and limiting devices,. there are three Dofs of the platform , as is stated above.

The platform comprises 1 Upper layer; 2 Springs; 3 Middle Raft; 4MSIs; 5 Base 6 Force Sensors; 7 Exciter motor. The actual parameters of the platform are: M_A=161.2kg，J_{Ax}=7.00kg*m^2， J_{Ay}=8.02kg*m^2； M_B=161.2kg， J_{Bx}=7.00kg*m^2， J_{By}=8.02kg*m^2；M_R=675.7kg， J_{Rx}=129.73kg*m^2， J_{RZ}=69.15kg*m^2， $\xi_A^u = 0.01$， $K_B^u = 120N/mm$， $\xi_B^u = 0.01$， $K^d = 450N/mm$， $\varsigma^d = 0.01$，l=0.6，m=0.4，a=0.3，b=0.3。The input force of the exciter is sinusoidal, the range of the frequency from 3Hz to 40Hz.

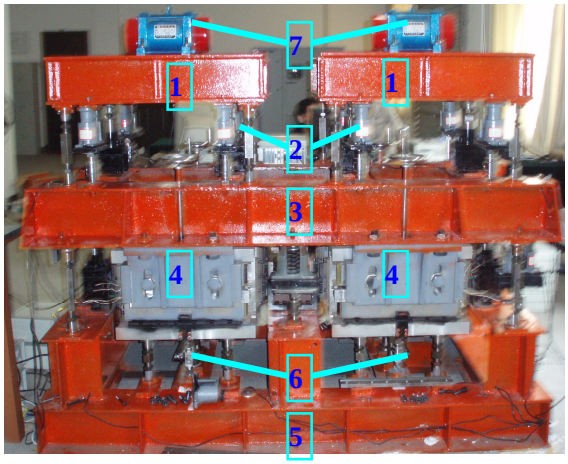

Figure 11 Physical picture of experimental platform
1 Upper layer; 2 Springs; 3 Middle Raft; 4MSIs; 5 Base; 6 Force Sensors; 7 Exciter motor

From the Force transmissibility curves in Fig12, we can see that the effect on vibration improves 2dB -3dB in low frequency, and it may be over up to 10dB -15dB, around resonance frequency. The test showed that the simulation result agrees well with test data.

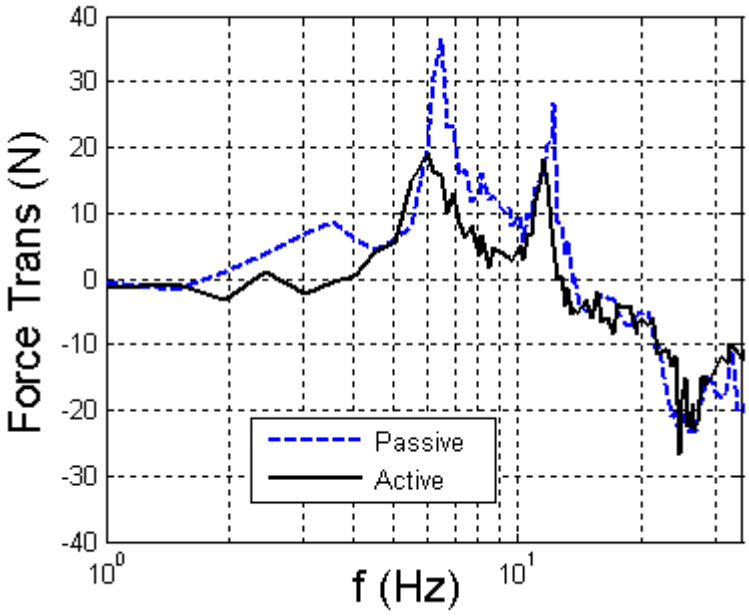

Figure 12. Force transmissibility of the two systems under experiment

6 Conclusion

Magnetic suspension supporting technology is applied to vibration isolation system. A multiple DOFs vibration isolation system that is supported by magnetic suspension isolators and ordinary springs is proposed. In order to avoid the shortcomings theoretical formula and increase the control precision, the actual magnetic force is measured and fitted by using least square methods.

A control model is established based on the minimum force transmissibility control strategy. The results of simulations show isolation performance of active vibration isolation system improves 2dB -3dB in lower frequency, is up to 18dB around the resonance frequencies. In order to prove the availability of the simulation model, the relative experiments is performed. The output forces and acceleration are measured by sensors, then The data are analyzed. The experimental results are found to be in good agreement with simulated results.

The research show that the active vibration isolation system has much better isolating performance against conventional passive isolation system in a very broad frequency range.

References

[1] Y. Liu, H. Matsuhisa, H. Utsuno, Semi-active vibration isolation system with variable stiffness and damping control.Journal of sound and vibration .2008.2(313):16-28

[2] K.G. Ahn, H.J. Pahk, M.Y. Jung, D.W. Cho,. A hybrid-type active vibration isolation system using neural networks . J.of Sound and Vibration, 1996, 192(4): 793-805.

[3] J. Leavitt, F. Jabbari, J.E. Bobrow. Optimal Performance of Variable Stiffness Devices for Structural Control. Journal of Dynamic Systems, Measurement, and Control MARCH 2007, Vol. 129 , 171-177

[4] Y. Liu, T.P. Waters, M.J. Brennan. Comparison of semi-active damping control strategies for vibration isolation of harmonic disturbances. Journal of Sound and Vibration 280 (2005) 21–39

[5] P Gardonio, SJ. Elliott. Active isolation of structural vibration on a multiple-degree-of-freedom system, Part 2; Effectiveness of active control strategies. J. of Sound and Vibration, 1997, 207 (1): 95-121.

[6] J Niu, K Song, CW. Lim. On active vibration isolation of floating raft system . Journal of Sound and Vibration, 2005, (285): 391-406.

[7] Y. Hu, Z. Zhou ,Z. Jiang. Basic theory and application of active magnetic bearing [M]. China Machine Press.2006.4 106-107

[8] Md.E. Hoque, M. Takasaki, Y.Ishino,T. Mizuno, Development of a three-axis active vibration isolator using zero-power contol, IEEE/ASME Transactions on Mechatronics, 11(4)(2006) 462-469

[9] J. Liu,He P. Tie S. Luo, et al. Design and performance research of new-style and high-powered counter-force actuator of electromagnetic drive.Noise and Vibration Control, 2006(12),6: 69-72

[10] W. Fan,Y. Guo, Y. Zhang, et al. Finite element analysis and dynamic characteristic test of an electromagnetic actuator .Noise and Vibration Control, 2008.6(3):27-28,88

[11] S Daley,. F.A. Johnson, J.B.Pearson, et al. Active vibration control for marine applications. Control Engineering Practice, 2004, (12) : 465-474.

[12] S Daley, J. Hatonen, D.H.Owens, Active vibration isolation in a "Smart Spring" mount using a repetitive control approach. Control Engineering Practice, 2006, 14(9): 991-997.

[13] C Song, Y Hu, Z Zhou. Semi-active fuzzy control for a floating raft isolation system with magnetic suspension supporting.Journal of vibration and shock. Vol.28.No.9 2009:30-32

[14] C Song, Z Zhou,Y. Hu, Semi-active Fuzzy Control for Multi-Dof Floating Raft Isolation System with Magnetic Suspension Isolators.2009 Asia-Pacific Power and Energy Engineering Conference Proceedings. March 28-31, 2009. .p 1458-1462

[15] Y. Zhang , Audrew G.Alleyne . Active Vibration Isolation of Multiple Dof Systems Using a Position-Tracking Approach.Proceedings of the American Control Conference Denver,Colorado June4-6,2003: 809-814

[16] C. Song, Y. Hu, Z. Zhou, Study on a Control Mechanism of Differential Magnetic Suspension Active Vibration Isolation System. Journal of vibration and shock.Vol.27.No.7 2010

Appendix A.

The value of the five matrices *A,B,C,D* and *E*

$$
A=\begin{bmatrix}
0 & 0 & 0 & 1 & 0 & 0 & 0 & 0 & 0 & 0 & 0 & 0 & 0 & 0 & 0 & 0 & 0 & 0 \\
0 & 0 & 0 & 0 & 1 & 0 & 0 & 0 & 0 & 0 & 0 & 0 & 0 & 0 & 0 & 0 & 0 & 0 \\
0 & 0 & 0 & 0 & 0 & 1 & 0 & 0 & 0 & 0 & 0 & 0 & 0 & 0 & 0 & 0 & 0 & 0 \\
\frac{-4k_A^{\mu}}{m_A} & 0 & 0 & \frac{-4c_A^{\mu}}{m_A} & 0 & 0 & 0 & 0 & 0 & 0 & 0 & 0 & \frac{4k_A^{\mu}}{m_A} & \frac{-8ak_A^{\mu}}{m_A} & 0 & \frac{4c_A^{\mu}}{m_A} & \frac{-8ac_A^{\mu}}{m_A} & 0 \\
0 & \frac{-4a^2k_A^{\mu}}{J_{Ax}} & 0 & 0 & \frac{-4a^2c_A^{\mu}}{J_{Ax}} & 0 & 0 & 0 & 0 & 0 & 0 & 0 & 0 & \frac{4a^2k_A^{\mu}}{J_{Ax}} & 0 & 0 & \frac{4a^2c_A^{\mu}}{J_{Ax}} & 0 \\
0 & 0 & \frac{-4b^2k_A^{\mu}}{J_{Ay}} & 0 & 0 & \frac{-4b^2c_A^{\mu}}{J_{Ay}} & 0 & 0 & 0 & 0 & 0 & 0 & 0 & 0 & \frac{4b^2c_A^{\mu}}{J_{Ay}} & 0 & 0 & \frac{4b^2c_A^{\mu}}{J_{Ay}} \\
0 & 0 & 0 & 0 & 0 & 0 & 0 & 0 & 0 & 1 & 0 & 0 & 0 & 0 & 0 & 0 & 0 & 0 \\
0 & 0 & 0 & 0 & 0 & 0 & 0 & 0 & 0 & 0 & 1 & 0 & 0 & 0 & 0 & 0 & 0 & 0 \\
0 & 0 & 0 & 0 & 0 & 0 & 0 & 0 & 0 & 0 & 0 & 1 & 0 & 0 & 0 & 0 & 0 & 0 \\
0 & 0 & 0 & 0 & 0 & 0 & \frac{-4k_B^{\mu}}{m_B} & 0 & 0 & \frac{-4c_B^{\mu}}{m_B} & 0 & 0 & \frac{4k_B^{\mu}}{m_B} & \frac{8ak_B^{\mu}}{m_B} & 0 & \frac{4c_B^{\mu}}{m_B} & \frac{8ac_B^{\mu}}{m_B} & 0 \\
0 & 0 & 0 & 0 & 0 & 0 & 0 & \frac{-4a^2k_B^{\mu}}{J_{Bx}} & 0 & 0 & \frac{-4a^2c_B^{\mu}}{J_{Bx}} & 0 & 0 & \frac{-4a^2k_B^{\mu}}{J_{Bx}} & 0 & 0 & \frac{4a^2c_B^{\mu}}{J_{Bx}} & 0 \\
0 & 0 & 0 & 0 & 0 & 0 & 0 & 0 & \frac{-4b^2k_B^{\mu}}{J_{By}} & 0 & 0 & \frac{4b^2c_B^{\mu}}{J_{By}} & 0 & 0 & \frac{-4b^2c_B^{\mu}}{J_{By}} & 0 & 0 & \frac{4b^2c_B^{\mu}}{J_{By}} \\
0 & 0 & 0 & 0 & 0 & 0 & 0 & 0 & 0 & 0 & 0 & 0 & 0 & 0 & 0 & 1 & 0 & 0 \\
0 & 0 & 0 & 0 & 0 & 0 & 0 & 0 & 0 & 0 & 0 & 0 & 0 & 0 & 0 & 0 & 1 & 0 \\
0 & 0 & 0 & 0 & 0 & 0 & 0 & 0 & 0 & 0 & 0 & 0 & 0 & 0 & 0 & 0 & 0 & 1 \\
\frac{4k_A^{\mu}}{m_R} & 0 & 0 & \frac{4c_A^{\mu}}{m_R} & 0 & 0 & \frac{4k_B^{\mu}}{m_R} & 0 & 0 & \frac{4c_B^{\mu}}{m_R} & 0 & 0 & \frac{-4(k_A^{\mu}+k_B^{\mu}+k^d)}{m_R} & \frac{8a(k_A^{\mu}-k_B^{\mu})}{m_R} & 0 & \frac{-4(c_A^{\mu}+c_B^{\mu}+c^d)}{m_R} & \frac{8a(c_A^{\mu}-k_A^{\mu})}{m_R} & 0 \\
\frac{-8ak_A^{\mu}}{J_{Rx}} & \frac{4a^2k_A^{\mu}}{J_{Rx}} & 0 & \frac{-8ac_A^{\mu}}{J_{Rx}} & \frac{4a^2c_A^{\mu}}{J_{Rx}} & 0 & \frac{8ak_B^{\mu}}{J_{Rx}} & \frac{-4a^2k_B^{\mu}}{J_{Rx}} & 0 & \frac{8ac_B^{\mu}}{J_{Rx}} & \frac{-4a^2c_B^{\mu}}{J_{Rx}} & 0 & \frac{8a(k_A^{\mu}-k_B^{\mu})}{J_{Rx}} & \frac{-20a^2(k_A^{\mu}+k_B^{\mu})-36a^2k^d}{J_{Rx}} & 0 & \frac{8a(c_A^{\mu}-c_B^{\mu})}{J_{Rx}} & \frac{-20a^2(c_A^{\mu}+c_B^{\mu})-36a^2c^d}{J_{Rx}} & 0 \\
0 & 0 & \frac{-4b^2k_A^{\mu}}{J_{By}} & 0 & 0 & \frac{-4b^2c_A^{\mu}}{J_{By}} & 0 & 0 & \frac{-4b^2k_B^{\mu}}{J_{By}} & 0 & 0 & \frac{4b^2c_B^{\mu}}{J_{By}} & 0 & 0 & \frac{-4b^2(k_A^{\mu}-k_B^{\mu})-4b^2k^d}{J_{Rx}} & 0 & 0 & \frac{-4b^2(c_A^{\mu}-c_B^{\mu})-4b^2c^d}{J_{Rx}}
\end{bmatrix}
$$

$$B=\begin{bmatrix} 0 & 0 & 0 & 0 \\ 0 & 0 & 0 & 0 \\ 0 & 0 & 0 & 0 \\ 0 & 0 & 0 & 0 \\ 0 & 0 & 0 & 0 \\ 0 & 0 & 0 & 0 \\ 0 & 0 & 0 & 0 \\ 0 & 0 & 0 & 0 \\ 0 & 0 & 0 & 0 \\ 0 & 0 & 0 & 0 \\ 0 & 0 & 0 & 0 \\ 0 & 0 & 0 & 0 \\ 0 & 0 & 0 & 0 \\ 0 & 0 & 0 & 0 \\ 0 & 0 & 0 & 0 \\ 0 & 0 & 0 & 0 \\ \frac{1}{m_R} & \frac{1}{m_R} & \frac{1}{m_R} & \frac{1}{m_R} \\ \frac{-l}{J_{Rx}} & \frac{l}{J_{Rx}} & \frac{-l}{J_{Rx}} & \frac{l}{J_{Rx}} \\ \frac{m}{J_{Ry}} & \frac{m}{J_{Ry}} & \frac{-m}{J_{Ry}} & \frac{-m}{J_{Ry}} \end{bmatrix} \quad D=\begin{bmatrix} 0 & 0 & 0 & 0 \\ 0 & 0 & 0 & 0 \\ 0 & 0 & 0 & 0 \\ 0 & 0 & 0 & 0 \\ 1 & 0 & 0 & 0 \\ 0 & 1 & 0 & 0 \\ 0 & 0 & 1 & 0 \\ 0 & 0 & 0 & 1 \end{bmatrix}$$

$$E=\begin{bmatrix} 0 & 0 & 0 & 0 & 0 & 0 \\ 0 & 0 & 0 & 0 & 0 & 0 \\ 0 & 0 & 0 & 0 & 0 & 0 \\ \frac{1}{m_A} & 0 & 0 & 0 & 0 & 0 \\ 0 & \frac{1}{J_{Ax}} & 0 & 0 & 0 & 0 \\ 0 & 0 & \frac{1}{J_{Ay}} & 0 & 0 & 0 \\ 0 & 0 & 0 & 0 & 0 & 0 \\ 0 & 0 & 0 & 0 & 0 & 0 \\ 0 & 0 & 0 & 0 & 0 & 0 \\ 0 & 0 & 0 & \frac{1}{m_B} & 0 & 0 \\ 0 & 0 & 0 & 0 & \frac{1}{J_{Bx}} & 0 \\ 0 & 0 & 0 & 0 & 0 & \frac{1}{J_{Bx}} \\ 0 & 0 & 0 & 0 & 0 & 0 \\ 0 & 0 & 0 & 0 & 0 & 0 \\ 0 & 0 & 0 & 0 & 0 & 0 \\ 0 & 0 & 0 & 0 & 0 & 0 \\ 0 & 0 & 0 & 0 & 0 & 0 \\ 0 & 0 & 0 & 0 & 0 & 0 \end{bmatrix}$$

$$C=\begin{bmatrix} 0 & 0 & 0 & 0 & 0 & 0 & 0 & 0 & 0 & 0 & 0 & 0 & k^d & -3ak^d & bk^d & c^d & -3ac^d & bc^d \\ 0 & 0 & 0 & 0 & 0 & 0 & 0 & 0 & 0 & 0 & 0 & 0 & k^d & 3ak^d & bk^d & c^d & 3ac^d & bc^d \\ 0 & 0 & 0 & 0 & 0 & 0 & 0 & 0 & 0 & 0 & 0 & 0 & k^d & 3ak^d & -bk^d & c^d & 3ac^d & bc^d \\ 0 & 0 & 0 & 0 & 0 & 0 & 0 & 0 & 0 & 0 & 0 & 0 & k^d & -3ak^d & -bk^d & c^d & -3ac^d & -bc^d \\ 0 & 0 & 0 & 0 & 0 & 0 & 0 & 0 & 0 & 0 & 0 & 0 & 0 & 0 & 0 & 0 & 0 & 0 \\ 0 & 0 & 0 & 0 & 0 & 0 & 0 & 0 & 0 & 0 & 0 & 0 & 0 & 0 & 0 & 0 & 0 & 0 \\ 0 & 0 & 0 & 0 & 0 & 0 & 0 & 0 & 0 & 0 & 0 & 0 & 0 & 0 & 0 & 0 & 0 & 0 \\ 0 & 0 & 0 & 0 & 0 & 0 & 0 & 0 & 0 & 0 & 0 & 0 & 0 & 0 & 0 & 0 & 0 & 0 \end{bmatrix}$$